I. Troch, F. Breitenecker, eds. ISBN 978-3-901608-35-3

A 2+1D MODEL OF A PROTON EXCHANGE MEMBRANE FUEL CELL WITH GLASSY-CARBON MICRO-STRUCTURES

J.O. Schumacher, J. Eller, G. Sartoris

Corresponding author: J.O. Schumacher, Zurich University of Applied Sciences, Institute of Computational Physics
Wildbachstrasse 21, 8401 Winterthur, Switzerland, juergen.schumacher@zhaw.ch

Abstract. A computationally efficient model of a proton exchange membrane (PEM) fuel cell is presented, based on a "2+1D" FEM modelling approach. This approach is suitable to take the high aspect ratio between the in-plane and the through-plane dimensions of fuel cells into account. The anode and cathode are included as 2D domains. The coupling between two opposing elements of the anodic and cathodic side is established by a nonlinear 1D model representing the membrane electrode assembly (MEA).

This one-dimensional boundary value problem problem is formulated using the computer algebra software Mathematica. The approach is based on the symbolic weak form expressions of a nonlinear system of partial differential equations. The integrands of the tangential element stiffness matrix and the element residual vector of the coupled FEM problem are computed analytically by use of computer algebra. Mathematica is utilised to convert these integrands to C code automatically. Numerical integration, assembly of the element matrices, and the solution of the resulting nonlinear equation system is accomplished in a numerical efficient code in the programming language C.

The 2+1D FEM model is applied to simulate a micro polymer electrolyte fuel cell without gas diffusion layers with an active area of $1 cm^2$. The gas flow-field of this fuel cell is made of micro-structured glassy carbon plates. Stationary and isothermal simulation results for operation at an average current density of $250 mA/cm^2$ are presented. An inhomogeneous distribution of the local electric current density in the fuel cell plane is found. This local current density is determined by the supply with reactant gases, membrane water content etc. The current density is lowest near the gas inlet, it increases to a maximum value in the cell center, and decreases towards the gas outlet. The minimum value of the current density near the gas inlet is due to a low value of the membrane humidification, i.e. the protonic conductivity in this region is lowest here. An increase of the membrane water content is found in the cell center.

1 Introduction

A PEM fuel cell transforms the chemical energy liberated during the electro-chemical reaction of hydrogen and oxygen to electrical energy. Physical processes in a PEM fuel cell include the transport of the gas species, water, heat, and electric charge. Oxygen is reduced on the cathode side, and hydrogen is oxidised on the anode side in the electro-chemical reactions. A comprehensive fuel cell model needs to take these coupled transport processes into account. Moreover, transport of the reactant gases (oxygen and hydrogen) to the catalyst layers is mostly established using flow-field channels of serpentine shape. This leads to a complex shape of the in-plane model domain of the fuel cell.

In this contribution the following challenges in PEM fuel cell modelling are addressed:

- The modelling of the transport processes and the electro-chemical reactions results in a highly nonlinear coupled system of PDEs.
- There is a high aspect ratio between the in-plane dimensions (cell area ca. $1 - 800\ cm^2$) and the through-plane dimensions (MEA and GDL thickness ca. $500\ \mu m$). Discretising the cell geometry in three dimensions results in a very high number of DOF variables, and thus complicates parameter studies.
- For the technical application the interaction between the single cells in a fuel cell stack are of great importance. The interaction between the single cells in a stack is due to mass transport of the reactant gases and water, charge transport, and heat transport.

2 2+1D model approach

In the framework of our "2+1D" approach the gas flow channels and bipolar plates of the anode and cathode are discretised in two dimensions. The coupling between the anodic and cathodic side is established by a 1D model representing the membrane electrode assembly (MEA). Coupling between the 1D model of the MEA and the 2D models is achieved by using the values of the degrees-of-freedom (DOF) variables of the 2D model as Dirichlet boundary conditions for the 1D model. The fluxes of the 1D field variables at the 1D boundaries are then used as additional source terms in the 2D continuity equations.

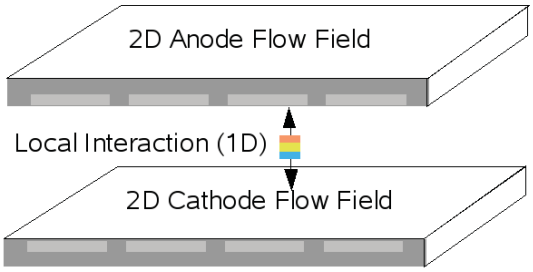

Figure 1: The 2D anodic and cathodic field variables of a PEM fuel cell are locally coupled with the 1D MEA model.

For a field variable u, the 2D balance equation is

$$\nabla \cdot j_{u,2D} = \Pi_{u,2D}(x,y)\,, \tag{1}$$

where $j_{u,2D}$ is the flux of u in the 2D domain, and $\Pi_{u,2D}(x,y)$ is a volume source term described by the 1D model of field variable u. In the 1D domain the flux $j_{u,1D}$ of field variable u is a flux to per area, a current density. Using the 2+1D coupling approach the 2D volume source $\Pi_{u,2D}(x,y)$ is described by the 1D current density j_u at the boundaries of the 1D domain by

$$\Pi_{u,2D}(x,y) = \frac{j_{u,1D}\cdot n}{t_u}\,, \tag{2}$$

where n is the outer normal of the 1D boundaries, and t_u is the virtual dimension of the 2D domain in z-direction according to field variable u. One can think of situations, where the virtual dimension t_u of a field variable u might differ from the virtual dimension t_v of a field variable v, as done in Section 3. There, the mass transport and the species transport of the gas flow in the channels of a flow field plate as well as the charge transport in the catalyst layer in touch with the flow field plate are described in one 2D domain using two different values of the virtual dimension t.

The 1D model of the membrane electrode assembly is created from the symbolic weak form expressions of the coupled transport phenomena. The tangential element stiffness matrix $T_{ij}^{(e)}$ and the element residual vector $R_i^{(e)}$

$$\begin{aligned} T_{ij}^{(e)} &= \frac{\partial R_i^{(e)}}{\partial u_j^{(e)}} \\ &= \frac{\partial}{\partial u_j^{(e)}}\left(\sum_m K_{im}^{(e)}\, u_m^{(e)} - f_i^{(e)}\right), \end{aligned} \tag{3}$$

$$R_i^{(e)} = \sum_j K_{ij}^{(e)}\, u_j^{(e)} - f_i^{(e)}\,, \tag{4}$$

of the coupled FEM problem are computed analytically by the computer algebra software Mathematica [6], where $K_{ij}^{(e)}$ is the element stiffness matrix, $u_i^{(e)}$ are the element DOF variables and $f_i^{(e)}$ is the element load vector. Since $T_{ij}^{(e)}$ and $R_i^{(e)}$ depend on the DOF variables $u_i^{(e)}$ we obtain a nonlinear system of equations.

The symbolic expressions of the integrands of the tangential stiffness matrix $T_{ij}^{(e)}$ and of the residual vector $R_i^{(e)}$ are converted to the programming language C by Mathematica and used to assemble the system matrix. Finally, a nonlinear coupled 2+1D problem is solved for with the FEM code SESES [3]. Thereby, the residual is composed of a contribution that stems from the 2D equations, and one contribution of the 1D problem

$$R_{u^{r,M}} = R^{2D}_{u^{r,M}} + R^{1D}_{\phi_0^r}(\phi_0^r, \phi_L^r)\,. \tag{5}$$

3 2D model of the flow-field plates

Convective and diffusive mass transport is accounted for in the plane of the main flow direction (in-plane). No mass transport is assumed to appear where the flow-field plates are in contact with the catalyst layers. Therefore, the mass transport equations are solved only in the 2D domains of the gas flow channels. Assuming potential flow conditions in the gas flow channels the velocity and pressure distribution can be described by a porous flow approach using Darcy's law

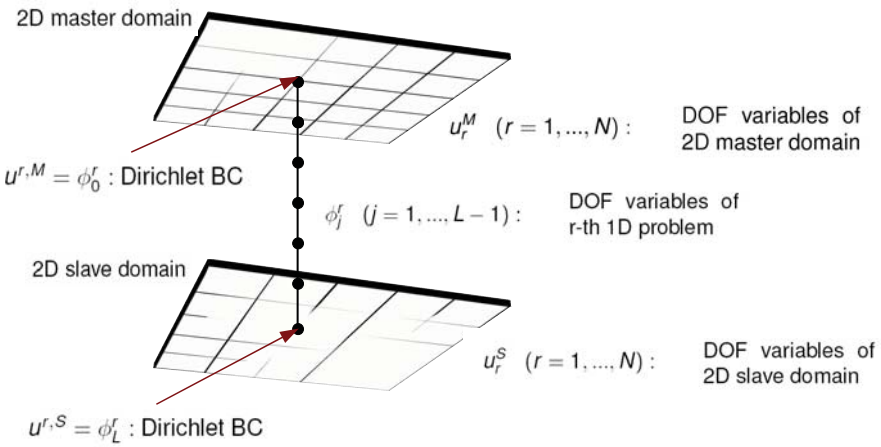

Figure 2: With the "2+1D" modelling approach all DOF-variables of a 2D master domain and the opposing 2D slave domain are coupled with a 1D model. The 2D DOF variable values $u^{r,M}$ and $u^{r,S}$ are used as Dirichlet boundary conditions ϕ_0^r and ϕ_L^r to solve a 1D FEM model. The fluxes of the 1D field variables at the 1D boundaries are used in additional source terms in the 2D continuity equations.

$$v = -\frac{\mu}{\kappa}\nabla P, \tag{6}$$

where μ is the viscosity of the gas mixture, and κ is the permeability of the porous material. The permeability was determined by fitting the simulated pressure difference between gas inlet and gas outlet to measurements [2]. The stationary 2D mass balance reads

$$\nabla \cdot (\rho v) = \Pi_m(x,y), \tag{7}$$

where $\Pi_m(x,y)$ is the total mass production rate described by the 1D-MEA model.

The stationary species balance equation for the species α is given by

$$\nabla \cdot (\rho_\alpha v) = -\nabla \cdot j_\alpha + \Pi_\alpha, \tag{8}$$

where ρ_α is the species mass density, $\rho = \sum_\alpha \rho_\alpha$ is the total mass density, j_α are the species diffusion currents, Π_α are the species production rates described by the 1D-MEA model, and $\Pi_m = \sum_\alpha \Pi_\alpha$ is the total mass production rate also described by the 1D-MEA model. Eq. 8 can be rewritten by using Eq. 7, this yields

$$\nabla\left(\frac{\rho_\alpha}{\rho}\right) \cdot \rho v = -\nabla \cdot j_\alpha + \Pi_\alpha(x,y) - \Pi_m(x,y)\frac{\rho_\alpha}{\rho}. \tag{9}$$

The species to be solved for are $\alpha_{\text{anode}} = \{H_2, H_2O\}$ at the anode, and $\alpha_{\text{cathode}} = \{O_2, H_2O\}$ at the cathode. To ensure that the sum of the molar fractions is one, the species production rate $\Pi_\alpha(x,y)$ of species α has to be corrected using the total mass production rate [3]. The species diffusion currents $j_\alpha = -\sum_\beta D_{\alpha\beta}\nabla x_\beta$ can eventually be described with multi-component diffusion according to the Stefan-Maxwell model.

In the 2D domains the in-plane charge transport in the catalyst layers is accounted for. Assuming ideal electrical contact between the flow-field plates and the catalyst layers, the edges of the flow-field plates define the electrical boundary conditions of the 2D domain. Therefore, in-plane charge transport is modelled only between the edges of the flow-field plates and the active catalyst layer domains. Charge transport in the in-plane direction is described by a potential equation

$$j(x,y) = -\sigma\nabla\Phi, \tag{10}$$

and the charge continuity equation

$$\nabla \cdot j(x,y) = \Pi_c(x,y), \tag{11}$$

where Φ is the electric potential of the catalyst layer, σ is the electrical conductivity of the catalyst layers in the in-plane direction, and $\Pi_c(x,y)$ is the contribution of the electrical current in the through-plane direction that is calculated by the 1D-MEA model.

The operating conditions and boundary conditions used for the 2D calculations are summarised in Table 1, and the material properties are given in Table 2.

4 One dimensional model of the membrane electrode assembly

Charge transport in the membrane electrode assembly is described by two potential equations for the electronically conducting phase ϕ_e, and the proton conducting phase ϕ_p [1]. Both equations are coupled by the source terms Q_A (Eq. 17) and Q_C (Eq. 18). These equations are the Butler-Volmer equations that describe the electrochemical reactions in the anodic catalyst layer Ω_A, and the cathodic catalyst layer Ω_C. In the membrane domain Ω_M the source terms in Eq. 14 and Eq. 15 are zero as there are no electrochemical reactions in the membrane. The current densities are given by

$$j_e(x) = -\sigma_e \nabla \phi_e(x)\,, \tag{12}$$

$$j_p(x) = -\sigma_p \nabla \phi_p(x)\,. \tag{13}$$

The continuity equations are

$$\nabla \cdot j_e(x) = q_e = \begin{cases} -Q_A & \text{in } \Omega_A \\ 0 & \text{in } \Omega_M \\ -Q_C & \text{in } \Omega_C \end{cases}, \tag{14}$$

$$\nabla \cdot j_p(x) = q_p\,. \tag{15}$$

Charge conservation is accounted for with the following equation

$$q_p = -q_e\,. \tag{16}$$

The source terms of the continuity equations Eq. 14 and Eq. 15 are

$$Q_A = i_{0A} \cdot S_a \cdot \frac{x_{H_2}}{x_{H_2}^{ref}} \cdot \left(\exp\left[\frac{(1-\alpha)F}{RT}(\phi_e - \phi_p) \right] - \exp\left[-\frac{\alpha F}{RT}(\phi_e - \phi_p) \right] \right), \tag{17}$$

$$Q_C = i_{0C} \cdot S_a \cdot \frac{x_{O_2}}{x_{O_2}^{ref}} \cdot \left(\exp\left[\frac{2(1-\alpha)F}{RT}(\phi_e - \phi_p - (\Delta\phi_c^0 - \eta_{OC})) \right] - \exp\left[-\frac{2\alpha F}{RT}(\phi_e - \phi_p - (\Delta\phi_c^0 - \eta_{OC})) \right] \right), \tag{18}$$

where i_{0A} and i_{0C} is the exchange current density on the anode side, and the cathode side, respectively. S_a relates the catalyst layer volume to the active catalyst layer surface, x_{H_2} is the anode hydrogen molar fraction, x_{O_2} is the cathode oxygen molar fraction, α is the symmetry factor, F the Faraday constant, R is the universal gas constant, T is the temperature, $\Delta\phi_c^0$ the equilibrium potential of the cathode reaction, and η_{OC} is the open circuit overpotential. The open circuit overpotential η_{OC} is used to describe the deviation between the theoretic equilibrium potential of the cathode reaction $\Delta\phi_c^0$ and the measurable open circuit voltage that is mainly caused by species diffusion through the membrane. The reference molar fractions of hydrogen on the anode side $x_{H_2}^{ref}$ and oxygen on the cathode side $x_{O_2}^{ref}$ are set to one.

The value of $(j_e/t_{CL}) \cdot n$ at the 1D boundaries is used as value of $\Pi_c(x,y)$ in the continuity equation of the electric potential (Eq. 11) in the 2D anode domain and the 2D cathode domain, where n is the outer normal of the 1D boundaries, and t_{CL} is the virtual dimension of the catalyst layers in the 2D domains in z-direction.

The molar fractions of hydrogen x_{H_2} and oxygen x_{O_2} are assumed to be constant in the catalyst layers. Therefore, the value of $\Pi_{H_2}(x,y)$ in the continuity equation of the hydrogen species (Eq. 9) in the 2D anode domain is calculated using Faraday's law by $[(j_e M_{H_2}/(2F)] \cdot n/t_{GAS}$, where F is the Faraday constant, M_{H_2} the molar mass of hydrogen, and t_{GAS} is the virtual dimension of the gas channels in the flow field plates in the 2D domains in z-direction. The value of $\Pi_{O_2}(x,y)$ in the continuity equation of the oxygen species (Eq. 9) in the 2D cathode domain is calculated similarly by $[-j_e M_{O_2}/(4F)] \cdot n/t_{GAS}$, where M_{O_2} is the molar mass of oxygen. $\Pi_{O_2}(x,y)$ is set to zero in the 2D anode domain, and $\Pi_{H_2}(x,y)$ is set to zero in the 2D cathode domain.

The model of the membrane electrode assembly also accounts for membrane water transport according to Springer [5]. The membrane water content λ is defined as the number of water molecules per sulfonic acid group of the membrane. The total water flux in the membrane $j_{\lambda,tot}$ can be described as a combination of electroosmotic water drag $j_{\lambda,drag}$ and diffusive water flux $j_{\lambda,diff}$

$$j_{\lambda,tot} = j_{\lambda,drag} + j_{\lambda,diff}\,, \tag{19}$$

$$j_{\lambda,tot} = n_{drag} \cdot \frac{\sigma_p(T,\lambda)\nabla\phi_p}{F} - \frac{\rho_{dry}}{M_M} \cdot D_\lambda \nabla\lambda, \tag{20}$$

where n_{drag} is the electroosmotic drag coefficient, $\sigma_p(T,\lambda)$ is the protonic conductivity of the membrane that depends on the temperature T and the membrane water content λ, ρ_{dry} is the density of the dry membrane, M_M is the equivalent weight of the membrane, and D_λ is the water diffusivity in the membrane. Therefore, the continuity equation

$$\nabla \cdot j_{\lambda,tot} = q_{H_2O}\,, \tag{21}$$

reads

$$\nabla \cdot \left[n_{drag} \cdot \frac{\sigma_p(T,\lambda)\nabla\phi_p}{F} \right] - \nabla \cdot \left[\frac{\rho_{dry}}{M_M} \cdot D_\lambda \nabla\lambda \right] = q_{H_2O}, \tag{22}$$

with the water production source term q_{H_2O} defined as

$$q_{H_2O} = \begin{cases} -Q_C(\phi_e,\phi_p,T)/2F & \text{in } \Omega_C \\ 0 & \text{otherwise} \end{cases}. \tag{23}$$

The boundary conditions of λ are calculated as a function of the water activity in the gas channels [5]. The protonic conductivity of the membrane is parameterised by

$$\sigma(T,\lambda) = exp\left[1268\left(\frac{1}{303}-\frac{1}{T}\right)\right]\cdot\sigma_{303K}(\lambda)\,, \tag{24}$$

$$\sigma_{303K}(\lambda) = 0.5139\lambda - 0.326\,, \tag{25}$$

where $\sigma_{303K}(\lambda)$ is the protonic conductivity at a temperature of 303 K.

The value of $j_{\lambda,tot} M_{H_2O} \cdot n/t_{GAS}$ at the 1D boundaries is used as value of $\Pi_{H_2O}(x,y)$ in the continuity equation of the water vapour species (Eq. 9) in the 2D anode domain and the 2D cathode domain, where M_{H_2O} is the molar mass of water.

As outlined in Section 2, the local 2D DOF variable values are used to specify the Dirichlet boundary conditions of the 1D electric potential ϕ_e and the 1D membrane water content λ. For the 1D protonic potential ϕ_p isolating Neumann boundary conditions are defined at both 1D boundaries. The material properties used in the 1D calculations are given in Table 2.

5 Simulation Results

The 2+1D modelling approach was applied to simulate a micro proton exchange membrane fuel cell. This type of fuel cell consists of two stainless steel end plates, in which the functions of electrical contact, gas supply to the flow-field micro-structures, temperature control and mechanical compaction are combined. In-between these steel plates, two micro-structured glassy carbon plates, which are separated by the catalyst-coated membrane, are fixed [4]. The gas flow-field is fabricated in the glassy carbon plates by two-dimensional laser ablation. In this paper a flow-field shape is analysed that consists of eleven parallel gas flow channels at the gas inlet and three parallel gas flow channels at the gas outlet as can be seen in Fig. 5. The flow-field is of serpentine shape, and the number of channels is reduced step-wise by merging of two parallel channels into one channel.

The distribution of the reactant gases is shown in Fig. 5. Oxygen and hydrogen are consumed in the electrochemical reaction, and the oxygen molar fraction decreases from 0.91 at the inlet (top right) to 0.69 at the outlet (top left). The hydrogen molar fraction is 0.92 at the inlet, it decreases to 0.78 at the outlet.

The molar fraction of water vapour can be seen in Fig. 6. Water is accumulated at the cathode side, the molar fraction of H_2O increases towards the cathode outlet. Accordingly, the water vapour saturation increases to 100% already near the inlet as shown in Fig. 7. This is to due electrochemical production of water. Water vapour saturation values increase to high values of 2.7 near the outlet on the cathode side, that is, the model predicts water condensation to occur first on the cathode side near the outlet. Comparable results could be obtained by neutron radiography on the operating fuel cell at Paul Scherrer Institute, Switzerland. The relative humidity at the gas inlets is set to ca. 80%. Under these conditions, the model predicts a low membrane water content of about 8 water molecules per sulfonic group near the gas inlet (Fig. 8). In the cathode domain, this value increases to about 18 near the cell center and further increases to 20 at the gas outlet. This is due to electrochemical production of water in the cathode catalyst layer and takeup of water by the membrane. The membrane water content on the anode domain increases also in the direction of the gas flow. This is because the diffusive water flux through the membrane from the cathode to the anode exceeds the water flux that is due to electro-osmotic drag of water through the membrane from the anode to the cathode (see right part of Fig. 10).

The electric current density of the 2D domains in the through-plane direction is shown in Fig. 9. This current density is predicted by the 1D model, that is, in the direction perpendicular to the cell area. The current density is zero where the flow field plates are in contact with the catalyst layers, because of the assumption of no mass

Operating condition	Value [unit]
Temperature	323 K
Voltage BCs	
Anode CL	0.00 V
Cathode CL	0.75 V
Gas composition anode	
Gas flow (dry H_2)	9 sccm
Pressure at intlet	120217 Pa
Pressure at outlet	101325 Pa
Relative humidity	76.3 %
Gas composition cathode	
Gas flow (dry O_2)	6 sccm
Pressure at inlet	117189 Pa
Pressure at outlet	101325 Pa
Relative humidity	82.2 %

Table 1: Operation conditions used in simulations. In the experimental and numerical setup the dry educt gas flows are controlled before humidification. At the gas inlets the flow rates and the molar fractions of the gas species are specified. At the gas outlets the pressure is given. The pressure at the gas inlets is a result of the 2+1D calculations. The electrical boundary condition values are used as Dirichlet boundary condition values at the edges of the flow field plates being in contact with the catalyst layers.

Symbol	Material property	Value	[Unit]
	2D calculations		
μ	Viscosity of the gas mixture	1.78E-5	Pa/s
κ	Permeability of the anode gas channels	1.4E-10	m^2
	Permeability of the cathode gas channels	1.8E-10	m^2
D_{H_2,H_2O}	Binary diffusion coefficients of hydrogen in water vapour	0.102982E-2	m^2/s
D_{O_2,H_2O}	Binary diffusion coefficients of oxygen in water vapour	0.302748E-3	m^2/s
σ	Electrical conductivity of the catalyst layers in in-plane direction	42	S/m
t_{CL}	Virtual dimension of anode catalyst layer in z-direction	4.0E-6	m
	Virtual dimension of cathode catalyst layer in z-direction	6.0E-6	m
t_{GAS}	Virtual dimension of gas channels in the flow field plates in z-direction	120.0E-6	m
	1D calculations		
σ_e	Electric conductivity (through-plane)	42	S/m
i_{0A}	Anode exchange current density	10000	A/m^2
i_{0C}	Cathode exchange current density	0.0078	A/m^2
S_a	Coefficient relating the catalyst layer volume to the active catalyst layer surface	1.1E7	m^3/m^2
α	Symmetry factor	0.5	-
$\Delta\phi_c^0$	Equilibrium potential of the cathode reaction	1.229	V
η_{OC}	Open circuit overpotential	0.2	V
$x_{H_2}^{ref}$	Reference molar fraction of anode hydrogen	1	-
$x_{O_2}^{ref}$	Reference molar fraction of cathode oxygen	1	-
n_{drag}	Electro-osmotic drag coefficient	1	-
ρ_{dry}	Density of the dry membrane	2000	kg/m^3
M_M	Equivalent weight of the membrane	1.1	kg/equiv
D_λ	Water diffusivity in the membrane	5.0E-10	m^2/s

Table 2: Material properties used in 2D and 1D numerical calculations.

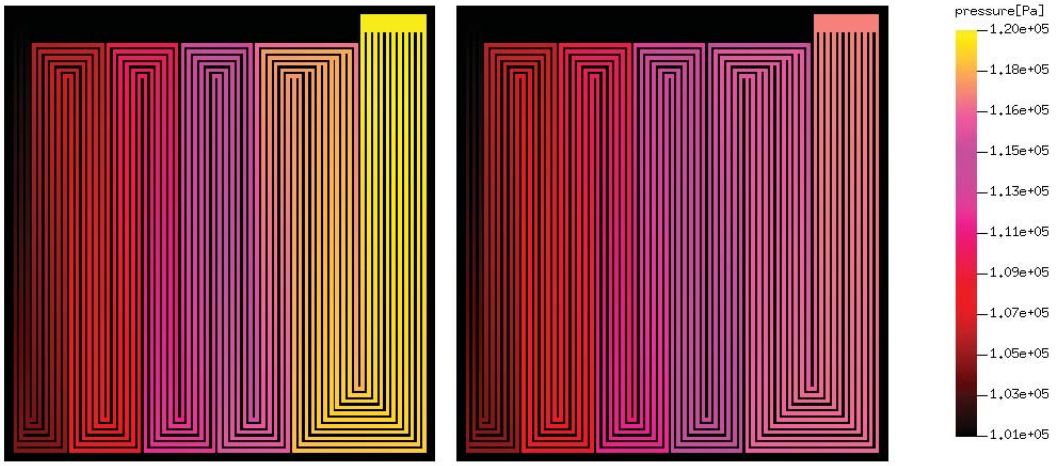

Figure 3: Pressure distribution in the flow-field channels (left: anode, right: cathode). At the gas inlets (top left of each domain) the flow rates and the molar fractions of the gas species are specified. At the gas outlets (top right of each domain) the pressure is given. The pressure at the gas inlets is a result of the 2+1D calculations.

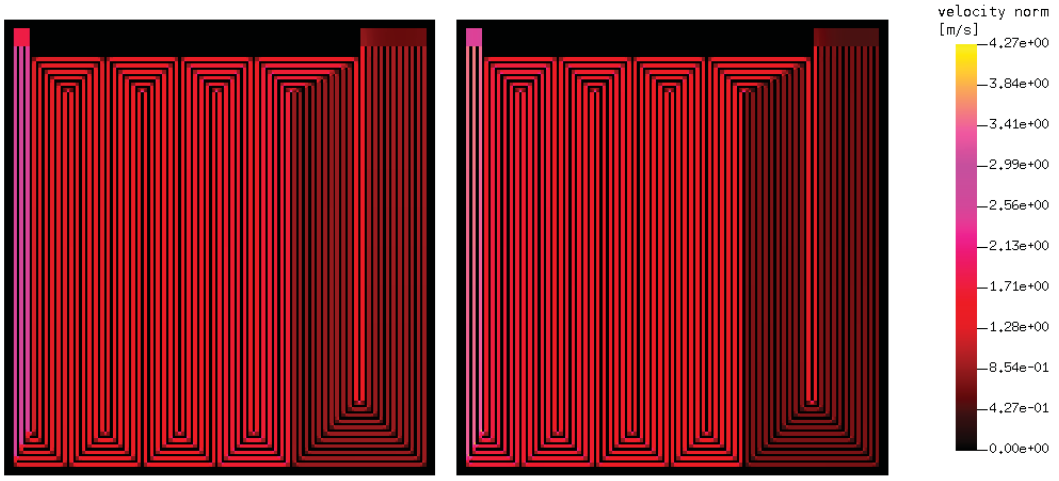

Figure 4: Absolute value of the gas velocity in the flow-field channels (left: anode, right: cathode).

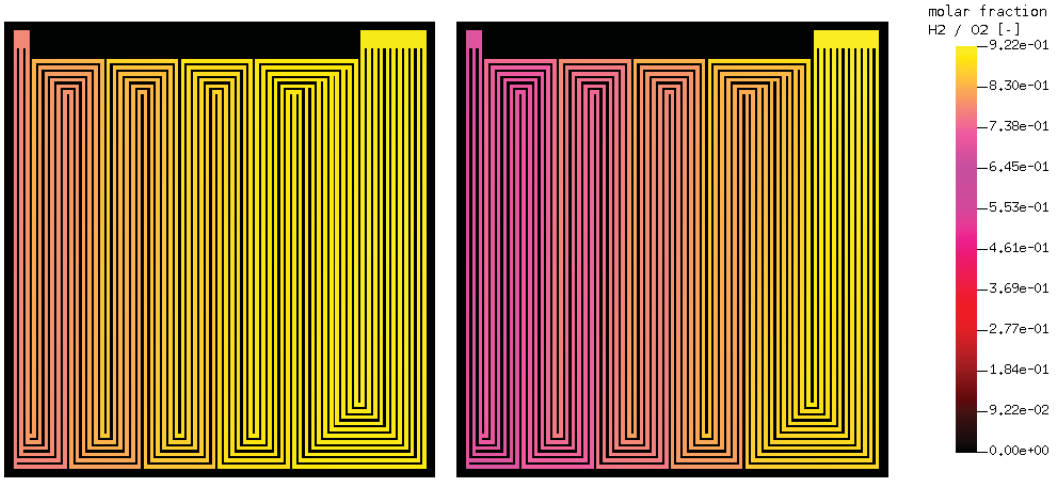

Figure 5: Molar fraction of H_2 and O_2 in the flow-field channels (left: anode, right: cathode).

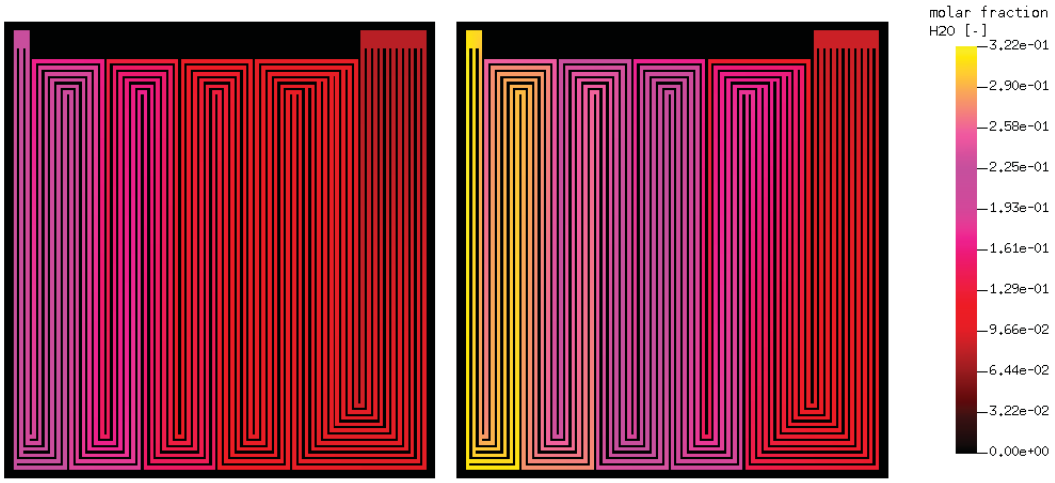

Figure 6: Molar fraction of H_2O in the flow-field channels (left: anode, right: cathode).

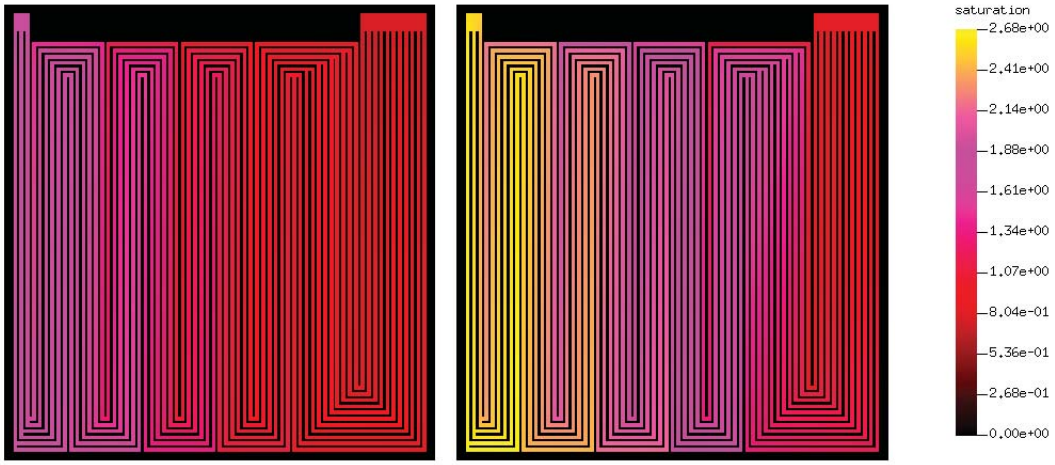

Figure 7: Water vapour saturation of the gas in the flow-field channels (left: anode, right: cathode).

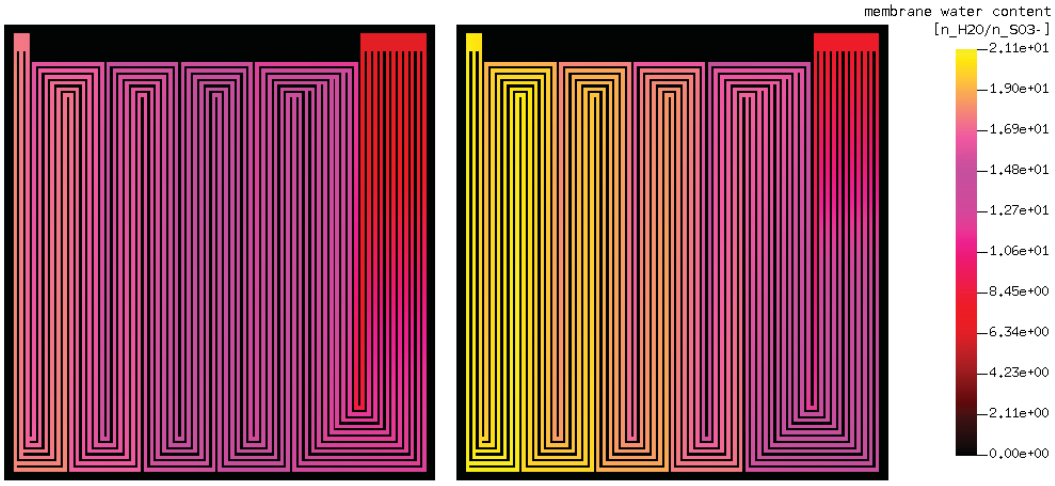

Figure 8: Membrane water content in number of water molecules per sulfonic acid group (left: anode, right: cathode).

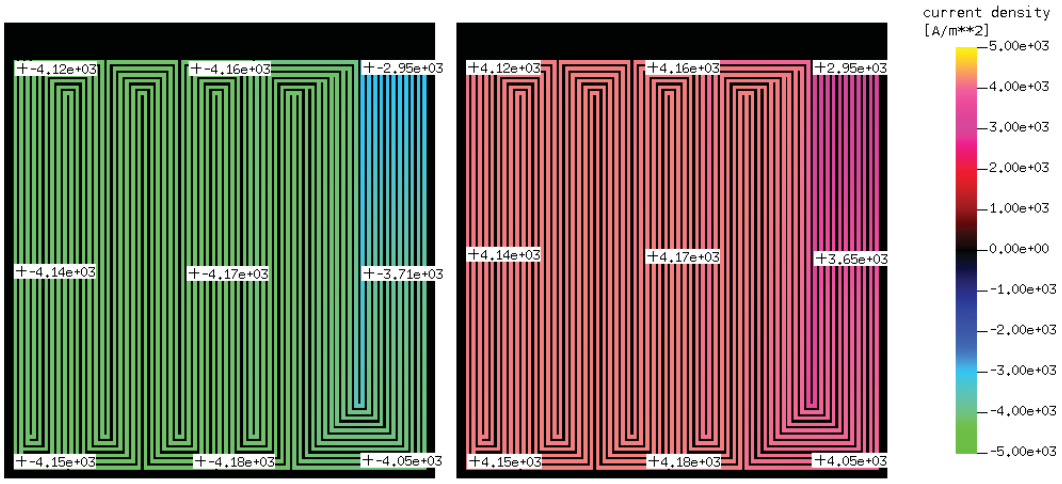

Figure 9: Electric current density in the through-plane direction as calculated by the 1D model, that is, in the direction perpendicular to the cell area (left: anode, right: cathode).

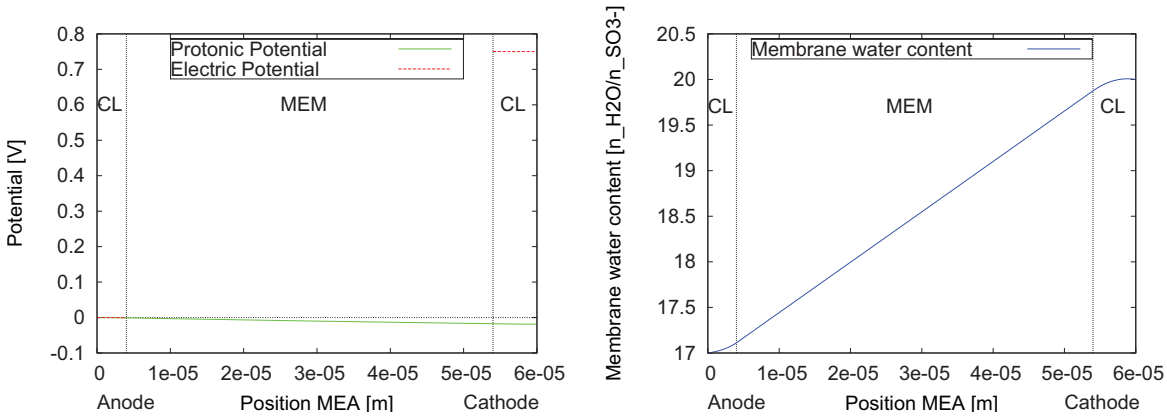

Figure 10: Conditions in the 1D MEA model near the outlets of the 2D gas flow channels. (left) Potential distribution of the electric and the protonic potential. The cathodic Dirichlet boundary condition is set to 0.75 V. This results in a current density of 401.2 mA/cm^2. The overpotential due to membrane resistance is abount 20mV. (right) Distribution of the membrane water content λ. The protonic current density in the anode catalyst layer (CL) increases towards the membrane. The increasing electro-osmotc drag of water in the anode CL towards the membrane leads to the curvature of λ in the anode CL. In the cathode CL the decreasing protonic current density and the electrochemical produced water are leading to a negative curvature of λ.

transport in the catalyst layers under the flow field plates. Positive charge is transferred from the anode to the cathode. Accordingly, a negative sign of the current density corresponds to a sink of the charge balance equation (left plot - anode), and a positive sign corresponds to a source of the charge balance equation (righ plot - cathode). The current density is lowest near the gas inlet (top right), it increases to a maximum value in the cell center, and decreases towards the gas outlet (top left). The minimum value of the current density near the gas inlet is due to a low value of the membrane humidification, i.e. the protonic conductivity in this region is lowest here. An increase of the membrane water content is found in the cell center.

The distribution of the electric and protonic potential in the 1D MEA model near the outlet of the gas flow channels is shown in the left part of Fig. 10. The distribution of the membrane water content in the 1D MEA model at the same position within the 2D domains is shown in the right part of Fig. 10.

6 Acknowledgements

The valuable input of Bernhard Seyfang of the Paul Scherrer Institute in Villigen (Switzerland) to this paper is gratefully acknowledged. The authors also wish to acknowledge the financial support by the GEBERT RÜF FOUNDATION in Switzerland.

7 References

[1] J. Newman and W. Tiedemann. Porous-electrode theory with battery applications. *AIChE*, 21:25, 1975.

[2] M. Roos, E. Batawi, U. Harnisch, and T. Hocker. Efficient simulation of fuel cell stacks with the volume averaging method. *Journal of Power Sources*, 118(1):86–95, 2003.

[3] G. Sartoris. Nm-seses tutorial: Finite element software for computer aided engineering, www.icp.zhaw.ch, 2008.

[4] B.C. Seyfang, M. Kuhnke, T. Lippert, G.G. Scherer, and A. Wokaun. A novel, simplified micro-pefc concept employing glassy carbon micro-structures. *Electrochemistry Communications*, 9:1958–1962, 2007.

[5] T. E. Springer, T. A. Zawodzinski, and S. Gottesfeld. Polymer electrolyte fuel cell model. *J. Electrochem. Soc.*, 138(8):2334–2342, 1991.

[6] S. Wolfram. Mathematica 7, www.wri.com, 2008.